Since January 2020 Elsevier has created a COVID-19 resource centre with free information in English and Mandarin on the novel coronavirus COVID-19. The COVID-19 resource centre is hosted on Elsevier Connect, the company's public news and information website.

Journal of Photochemistry & Photobiology, B: Biology 234 (2022) 112531

Contents lists available at ScienceDirect

Journal of Photochemistry & Photobiology, B: Biology

journal homepage: www.elsevier.com/locate/jphotobiol

UV-C irradiation-based inactivation of SARS-CoV-2 in contaminated porous and non-porous surfaces

Ana L. Tomás [a,1], Anna Reichel [a,1], Patrícia M. Silva [a,1], Pedro G. Silva [b,c], João Pinto [d], Inês Calado [d], Joana Campos [d], Ilídio Silva [d], Vasco Machado [d], Roberto Laranjeira [d], Paulo Abreu [d], Paulo Mendes [b,c], Nabiha Ben Sedrine [b,c], Nuno C. Santos [a,*]

[a] Instituto de Medicina Molecular, Faculdade de Medicina, Universidade de Lisboa, 1649-028 Lisbon, Portugal
[b] Castros S. A., 4410-160 São Félix da Marinha, Portugal
[c] MATGLOW, 4500-078 Espinho, Portugal
[d] CeNTI - Centre for Nanotechnology and Smart Materials, 4760-034 Vila Nova de Famalicão, Portugal

ARTICLE INFO

Keywords:
SARS-CoV-2
COVID-19
UV-C irradiation
Viral inactivation
Porous surfaces
Non-porous surfaces

ABSTRACT

The SARS-CoV-2 pandemic emphasized effective cleaning and disinfection of common spaces as an essential tool to mitigate viral transmission. To address this problem, decontamination technologies based on UV-C light are being used. Our aim was to generate coherent and translational datasets of effective UV-C-based SARS-CoV-2 inactivation protocols for the application on surfaces with different compositions. Virus infectivity after UV-C exposure of several porous (bed linen, various types of upholstery, synthetic leather, clothing) and non-porous (types of plastic, stainless steel, glass, ceramics, wood, vinyl) materials was assessed through plaque assay using a SARS-CoV-2 clinical isolate. Studies were conducted under controlled environmental conditions with a 254-nm UV-C lamp and irradiance values quantified using a 254 nm-calibrated sensor. From each material type (porous/non-porous), a product was selected as a reference to assess the decrease of infectious virus particles as a function of UV-C dose, before testing the remaining surfaces with selected critical doses. Our data show that UV-C irradiation is effectively inactivating SARS-CoV-2 on both material types. However, an efficient reduction in the number of infectious viral particles was achieved much faster and at lower doses on non-porous surfaces. The treatment effectiveness on porous surfaces was demonstrated to be highly variable and composition-dependent. Our findings will support the optimization of UV-C-based technologies, enabling the adoption of effective customizable protocols that will help to ensure higher antiviral efficiencies.

1. Introduction

Severe acute respiratory syndrome coronavirus 2 (SARS-CoV-2), which causes coronavirus disease 2019 (COVID-19), has emerged as a serious threat to human health worldwide. Although vaccination is reaping its rewards, the emergence of new variants of concern (VoC), along with the risk of future pandemics, emphasizes the need to devise additional efficient defence tools to mitigate viral spread.

SARS-CoV-2 can remain viable for several days on surfaces under controlled experimental conditions [1–3], causing a risk of transmission *via* smear infection and inhalation when the virus on these surfaces becomes airborne again [4–6]. These findings emphasize the importance of surface and environmental disinfection to reduce the risk of SARS-CoV-2 transmission. Devices based on ozone-free ultraviolet C (UV-C) germicidal radiation (peak emission at 254 nm) are in the spotlight, as they are an affordable and environment-friendly way to inactivate SARS-CoV-2 on contaminated surfaces, limiting viral spread in the current health crisis [4]. UV-C inactivates SARS-CoV-2 through viral genome damage, leading to the disruption of viral replication [7] and supports the value of UV-C irradiation against all VoC.

Although effectiveness of UV-C disinfection on SARS-CoV-2 has been reported [8–16], data that can be better translated from laboratory conditions to everyday life are needed. Data translation is limited because SARS-CoV-2 viability on surfaces depends on several parameters, such as the material, environmental conditions, and the deposition medium [17,18]. Moreover, challenges and intricacies of UV-C

* Corresponding author.
E-mail address: nsantos@fm.ul.pt (N.C. Santos).
[1] These authors contributed equally to the study.

https://doi.org/10.1016/j.jphotobiol.2022.112531
Received 16 May 2022; Received in revised form 11 July 2022; Accepted 20 July 2022
Available online 23 July 2022

measurements can stymie study translation when UV-C dose is not properly quantified.

In this work, our aim was to generate consistent, complete, reliable, and translational datasets of the use of UV-C irradiation as an effective neutralizing tool against SARS-CoV-2 on materials used in daily life. Virus infectivity after UV-C exposure of different well-characterized porous and non-porous surfaces was evaluated through plaque assay, using a SARS-CoV-2 clinical isolate. Antiviral activity was assessed by inoculating all surfaces with an infectious virus particle number resembling viral loads naturally present on contaminated surfaces [11]. Environmental conditions (temperature and humidity) were recorded, as they influence SARS-CoV-2 response to UV-C irradiation [19,20], and UV-C doses were precisely quantified using a 254 nm-calibrated sensor. A better understanding of UV-C effects on SARS-CoV-2, considering all key factors involved in the experimental setting, will allow result replication with different devices and in real-life environments. By addressing efficient disinfection protocols that can be adopted for materials present in shared environments such as hospitals, commercial spaces, schools, or public transportation, our findings can help to decrease SARS-CoV-2 dissemination and reduce the risk of related outbreaks in the future.

2. Materials and Methods

2.1. Tested Material

The effectiveness of UV-C irradiation on SARS-CoV-2 inactivation was evaluated for different porous and non-porous surfaces present in shared environments, namely hospitals, schools, and public transportation. Representative sample images are displayed in Fig. S1-S2. Composition, dimensions, and suppliers of the tested material are listed in Table S1.

2.2. Sample Preparation

All porous surfaces were cut into squares of 20 mm × 20 mm and a total weight of 0.4 ± 0.05 g was used per sample. Their sterilization was performed prior to each assay by autoclaving at 121°C for 15 min. Non-porous surfaces were used in the provided dimensions. All autoclaving-sensitive surfaces (plastics and floorings) were sterilized by immersion in 70% ethanol for 30 min under sterile conditions. Polystyrene (PS) samples were obtained already sterile.

2.3. UV-C Irradiation Source

In this work, a UV-C OSRAM 15 W ozone-free germicidal mercury vapor lamp was used. Prior to each UV-C inactivation procedure, the lamp was pre-heated for 6.5 min for warm-up and temperature stabilization. For each experiment, the parameters corresponding to UV-C irradiance (UV-C radiation intensity at the sample surface), exposure time and dose were quantified using a 254 nm-calibrated SGLUX wireless cosine-corrected UV sensor, together with its receiver unit (detection range from 0.009 to 9 W/m^2). Environmental conditions, *i.e.*, room temperature and relative humidity, were recorded using a datalogger

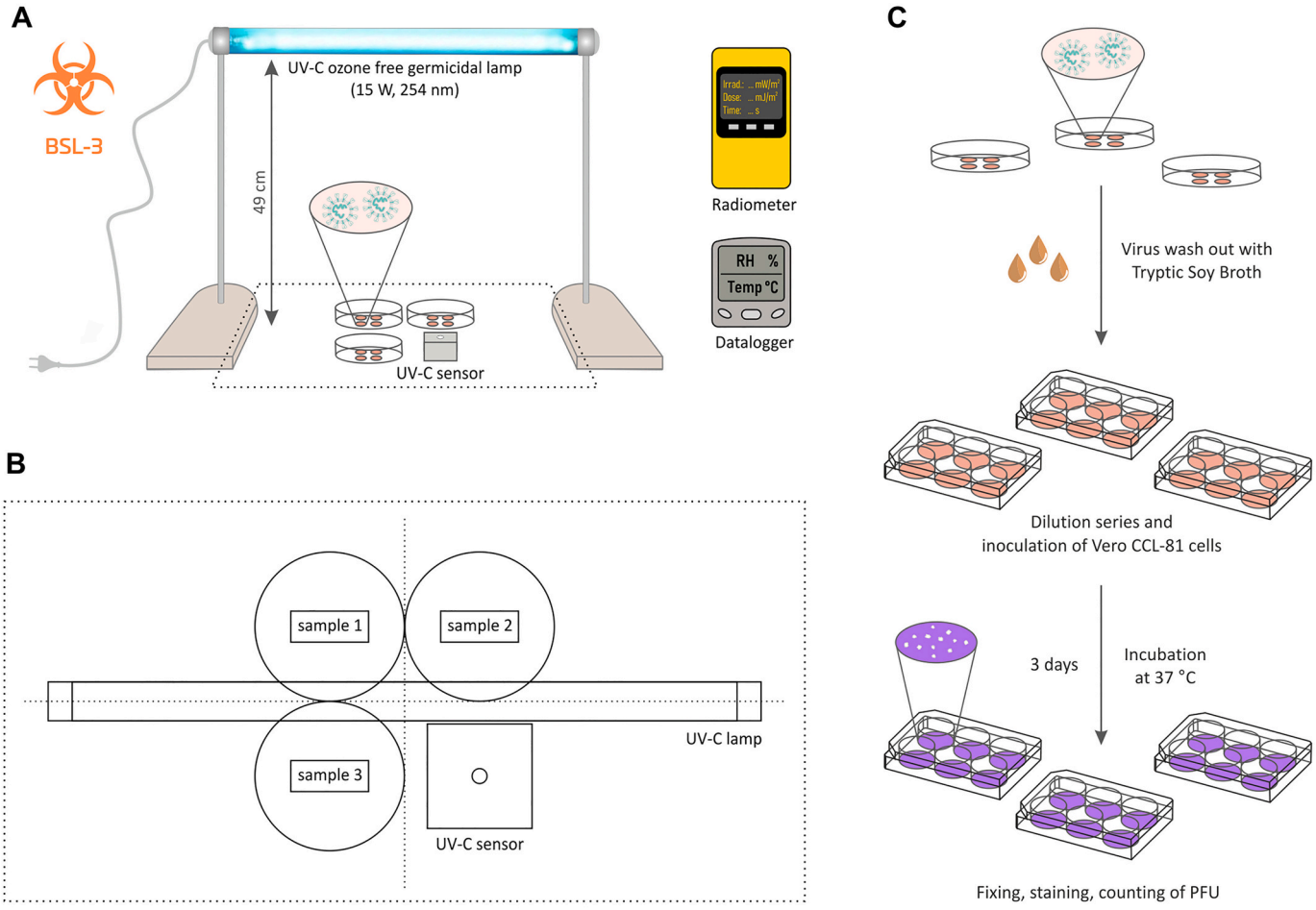

Fig. 1. (A) Scheme illustrating the positioning of samples, UV-C source, and measurement devices (UV-C sensor and datalogger) during UV-C treatment. (B) Top view of sample and sensor setup during treatment, showing their central positioning underneath the UV-C lamp (dashed area in A). (C) Main steps to quantify infectious virus particles, including sample washing and dilution steps, SARS-CoV-2 inoculation of Vero cell monolayers and reading of plaque assay results.

Ebro EBI 20. During treatment, the UV-C lamp was positioned 49 cm centrally above the samples and UV-C sensor, as shown in Fig. 1A-B.

2.4. Host Cells and SARS-CoV-2 Propagation

A viral stock of SARS-CoV-2 was generated from a strain previously isolated from a nasopharyngeal and oropharyngeal swab that tested positive by RT-qPCR (BioProject PRJEB38351; READS ENA ACCESSION ERR4157960) and was kindly provided by Prof. Pedro Simas (Instituto de Medicina Molecular). This viral stock was generated based on a previous protocol, with slight modifications [21]. Vero cells (ATCC, CCL-81) were used as a host organism and seeded one day prior to inoculation in T175 flasks using cell growth medium [Dulbecco's modified Eagle's medium (DMEM) supplemented with 10% heat-inactivated fetal bovine serum (HI-FBS), 50 U/mL penicillin, 50 μg/mL streptomycin, and 2 mM glutamine], to reach ~80–90% confluency the following day. The next day, cells were inoculated with an MOI of 0.02 of infectious SARS-CoV-2 and incubated for 2 h with gentle mixing every 15 min at 37°C with 5% CO_2. Subsequently, the inoculum was removed, substituted with 20 mL of fresh maintenance medium, and incubated for 4 days at 37 °C with 5% CO_2. Virus stocks were harvested by collecting supernatants after centrifugation (4°C, 290 X *g*, 5 min). The cleared supernatants were combined and mixed well before being aliquoted and cryopreserved at −80°C. The infectivity titre of the virus stock was assessed through plaque assay.

2.5. Virus Sample Preparation and UV-C Inactivation Procedure

Samples of porous and non-porous surfaces were placed in sterile Petri dishes and inoculated with 1.6×10^5 SARS-CoV-2 plaque forming units (PFU), a titre indicated as naturally occurring on contaminated surfaces [11], using a high titre virus stock ($\geq 1 \times 10^6$ PFU/mL). After inoculation, samples and UV-C sensor were subjected to UV-C irradiation until the desired dose was reached. Remaining infectious virus particles were recovered from non-porous and porous samples using 10 mL and 20 mL of washing solution (tryptic soy broth with 0.07% lecithin and 0.5% polysorbate 80), respectively. Porous samples were additionally agitated 5 times in a Vortex mixer for 5 s. Afterwards, 10-fold serial dilutions were prepared by transferring 200 μL of washed solution to 1.8 mL of cell maintenance medium (DMEM supplemented with 2.5% HI-FBS, 50 U/mL penicillin, 50 μg/mL streptomycin, and 2 mM glutamine), until a 10^{-3} dilution was reached. The recovered infectious virus particles were quantified by plaque assay. A scheme illustrating the quantification of remaining infectious virus particles after the inactivation protocol is displayed in Fig. 1C. In parallel, control samples from each surface were inoculated with the same SARS-CoV-2 stock suspension but not subjected to UV-C treatment. In these samples, washing occurred right after virus inoculation and recovered infectious virus particles were quantified by plaque assay to assess infectivity titres in the absence of UV-C treatment. All experiments were performed in triplicates, in a certified Biological Safety Level 3 (BSL-3) laboratory, following international and internal safety guidelines.

2.6. Determination of SARS-CoV-2 Inactivation by Plaque Assay

After every UV-C inactivation procedure, the recovered infectious virus particles from each tested sample were quantified by plaque assay. Vero cell monolayers seeded in 6-well plates were inoculated in duplicates with 500 μL of 10-fold serial dilutions (10^{-1},10^{-2},10^{-3}) performed with the washed-out virus suspension. Cells were incubated for 1 h with 5% CO_2, at 37 °C, with gentle rocking every 15 min. Subsequently, virus inoculum was removed and 2 mL of overlay medium (maintenance medium supplemented with 1% carboxymethyl cellulose) were added to the cell monolayer. After 3 days of incubation, overlay medium was removed, cells were fixed with 4% formaldehyde in PBS and stained with 0.05% toluidine blue to visualize viral plaques. The virus titre was calculated as plaque forming units/mL (PFU/mL), according to:

$$\frac{PFU}{mL} = plaque\ count\ mean \times \frac{1}{dilution} \times \frac{1}{inoculum} \quad (1)$$

where *plaque count mean* is the average number of plaques counted in all triplicates, *dilution* is the dilution at which the plate count was made, and *inoculum* is the volume (in mL) of washed-out virus used to perform the plaque assay. Under these experimental conditions, the limit of detection in the plaque assay was considered 1 PFU at the lowest dilution tested (10^{-1}). The antiviral activity (M_v) of the UV-C irradiation process was calculated from the relation between the UV-C treated samples and the control samples, according to:

$$M_v = log\ (V_a) - log(V_b) \quad (2)$$

where $\log(V_a)$ and $\log(V_b)$ are the decimal logarithm averages of 3 infectivity titre values after inoculation of the respective control samples and samples following UV-C treatment, respectively. Finally, the percentage of viral activity reduction ($R_{\%}$) was calculated as:

$$R_{\%} = \left(1 - \frac{1}{10^{M_v}}\right) \times 100 \quad (3)$$

2.7. UV-C Inactivation Studies

UV-C inactivation studies were performed in two phases. In phase I, one representative sample of each surface type (porous/non-porous) was selected and analysed. The relation UV-C dose *versus* recovered infectious virus particles and viral activity reduction ($R_{\%}$) was determined. In this phase, 8 dose values (from 1 to 8 mJ/cm^2) and 12 dose values (from 7 to 528 mJ/cm^2) were tested with the selected non-porous and porous surface, respectively, until the plaque assay detection limit was reached. The critical doses corresponding to an efficient treatment (1- to 3-log reduction) for both surfaces were then determined from dose-response analyses. In phase II, remaining non-porous surface samples were treated with the critical dose determined in phase I. Considering the different composition of the remaining porous surface samples and its implication in achieving effective UV-C irradiation doses, assays included at least 3 critical doses (132, 264 and 396 mJ/cm^2), also determined in phase I.

2.8. Data Analysis

Statistical analysis was performed at a $p < 0.05$ significance level, using Prism 8 (GraphPad Software, La Jolla, CA, USA). Spearman's correlation coefficients (r_s) were used to measure the magnitude of the association, or correlation, and the direction of the relationship between the UV-C dose and the viral activity reduction percentage obtained after each inactivation protocol.

3. Results

Antiviral assays were performed in two phases. In phase I, a dose-response assessment for each surface type was performed on representative samples to identify critical doses for an efficient UV-C treatment. In phase II, the determined critical doses were applied to the remaining surfaces.

3.1. Phase I: Dose-Response Studies on Selected Porous and Non-Porous Surfaces

Polystyrene Petri dishes were used as a representative sample for non-porous surfaces. These were subjected to increasing UV-C irradiation doses (1–8 mJ/cm^2). The corresponding dose-response behaviour is represented in Fig. 2, showing the decrease of infectious virus particle numbers with increasing UV-C doses. Additional information, including

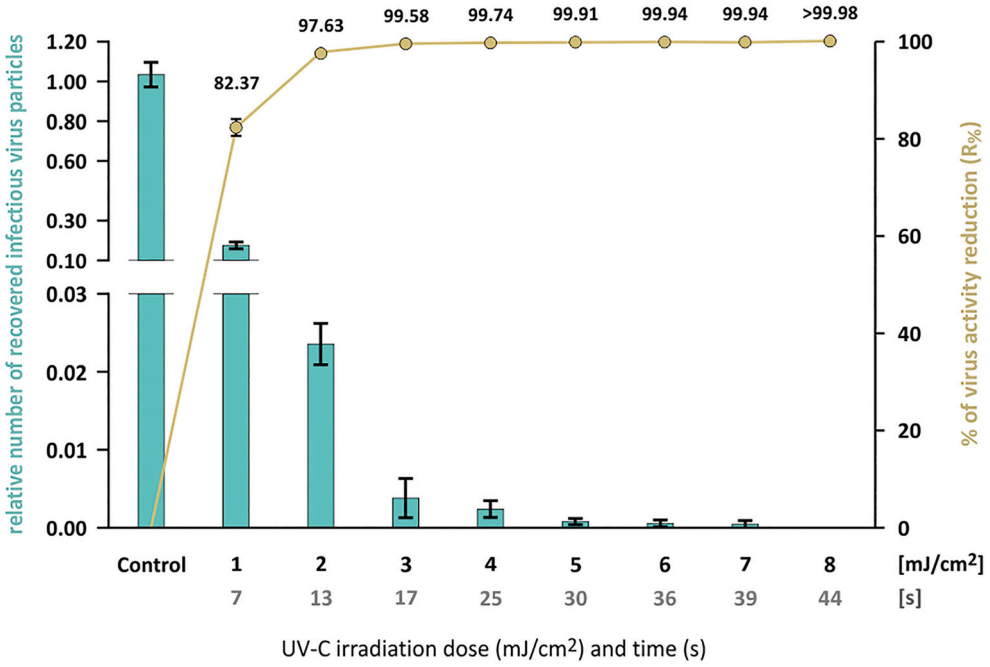

Fig. 2. Dose-response behaviour for polystyrene samples (representative non-porous surface). Bars represent infectious virus particles numbers recovered from the sample after respective irradiation times in relation to the control (no UV-C exposure). Yellow dots and line represent corresponding percentages of viral inactivation. Data are presented as mean ± standard deviation. (For interpretation of the references to colour in this figure legend, the reader is referred to the web version of this article.)

recorded UV-C irradiance, exposure times and environmental conditions during the experiments, are listed in Table 1. These results demonstrate a strong positive monotonic correlation between UV-C dose and $R_{\%}$ (r_s = 0.994; $p \leq 0.0001$). The dose required to achieve 1-log (90%) and 2-log (99%) reduction in SARS-CoV-2 activity on the tested non-porous sample is below 2 and 3 mJ/cm^2, respectively. Furthermore, a guaranteed 3-log (99.9%) reduction is achieved in <40 s, using a critical UV-C dose equal to or higher than 6 mJ/cm^2.

Car upholstery was selected as a reference sample for porous surfaces. Samples were subjected to increasing UV-C irradiation doses (7–528 mJ/cm^2), shown in Fig. 3 and Table 2. These results demonstrate a strong positive monotonic correlation between UV-C dose and $R_{\%}$ (r_s = 0.993; $p \leq 0.0001$). The critical dose to achieve 1-log (90%) reduction in SARS-CoV-2 activity on the tested porous sample is between 132 and 198 mJ/cm^2, requiring a minimum exposure time between 9 and 14 min. To guarantee 2-log (99%) reduction, the critical UV-C dose needs to be increased to 528 mJ/cm^2, representing an exposure time of 37 min. For the present study, exposure times higher than 37 min were not analysed, since polymers break down and textile compounds degrade over time during UV exposure [22,23]. Therefore, a 3-log reduction was not reached with the tested doses under the chosen experimental settings.

Phase I results illustrate that for both surface types higher UV-C irradiation doses (*i.e.*, longer exposure times) result in a larger reduction of remaining active SARS-CoV-2 particles. Yet, an efficient reduction of infectious virus particle numbers was achieved more rapidly and at lower doses for non-porous surfaces, when compared to porous surfaces.

We used a mathematical method based on the Weibull Model [24] that can precisely fit photoinactivation kinetics data and extract the lethal dose required for any level of inactivation (Fig. 4). This method enables the calculation of the tolerance factor, T, a dimensionless parameter that indicates the overall inactivation rate behaviour. Applying this formalism, we obtained lethal doses for 90% (LD_{90}) of 0.85 mJ/cm^2 and 119.2 mJ/cm^2, as well as T values of 0.61 and 0.51 for polystyrene and car upholstery, respectively. These parameters are relevant for data standardization, in order to facilitate the comparison of the inactivation kinetics between different studies or different microorganisms.

3.2. *Phase II: Applying Critical UV-C Doses on Remaining Porous and Non-Porous Surfaces*

To know if a single critical dose could be implemented to guarantee a highly efficient SARS-CoV-2 inactivation (3-log reduction) on all selected non-porous surfaces, the highest tested dose in phase I (8 mJ/cm^2) was applied to the remaining samples. All experimental conditions and inactivation results are presented in Table 3. These results demonstrate that 8 mJ/cm^2, corresponding to an exposure time > 1 min, were enough to ensure 3-log reduction of SARS-CoV-2 activity on all tested

Table 1
UV-C doses assessed for their antiviral activity on polystyrene (non-porous surface) with recorded UV-C irradiances, exposure times and environmental conditions (relative humidity, temperature). Corresponding antiviral activity (M_v) and percentage of viral activity reduction ($R_{\%}$) are presented as mean ± standard deviation.

Sample	Dose (mJ/cm^2)	Irradiance (mW/cm^2)	Exposure time (s)	RH (%)	Temperature (°C)	M_v	$R_{\%}$ (%)
Polystyrene	1	0.18	7	61–62	20–21	0.76 ± 0.04	82.37 ± 1.73
	2	0.18	13	57–58	20–21	1.63 ± 0.05	97.63 ± 0.27
	3	0.19	17	41–43	22–24	2.50 ± 0.37	99.58 ± 0.27
	4	0.19	25	44–45	21–24	2.62 ± 0.22	99.74 ± 0.11
	5	0.19	30	45–49	21–24	3.12 ± 0.24	99.91 ± 0.04
	6	0.20	36	45–49	21–24	3.28 ± 0.29	99.94 ± 0.04
	7	0.20	39	46–50	21–24	3.39 ± 0.37	99.94 ± 0.04
	8	0.20	44	44–45	21–22	>3.62*	>99.98*

RH – Relative humidity; * – No infectious virus particles were recovered after UV-C treatment, a value above the detection limit was assumed.

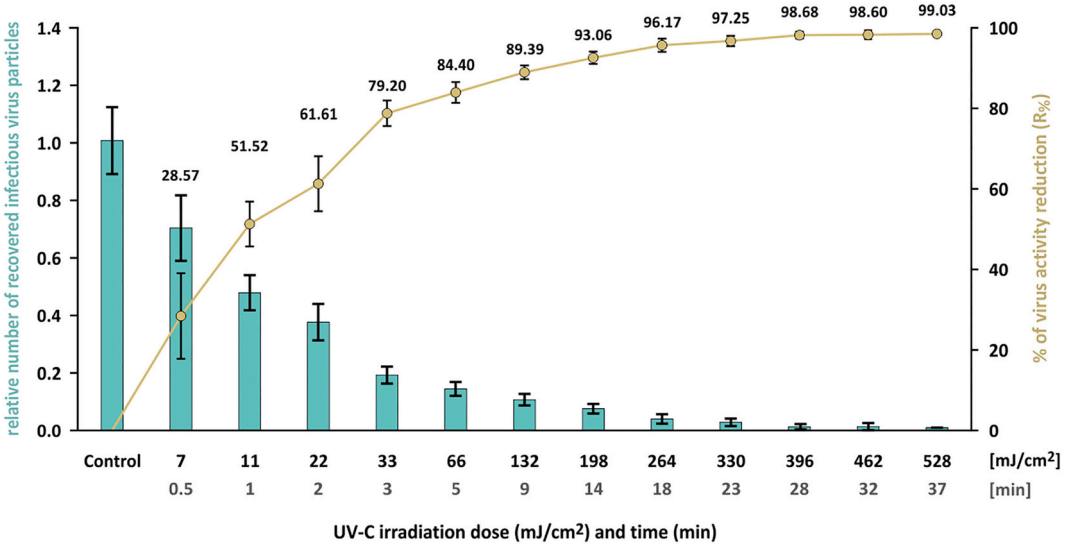

Fig. 3. Dose-response behaviour for car upholstery samples (representative porous surface). Bars represent infectious virus particle numbers recovered from the sample after respective irradiation times in relation to the control (no UV-C exposure). Yellow dots and line represent corresponding percentages of viral inactivation. Data are presented as mean ± standard deviation. (For interpretation of the references to colour in this figure legend, the reader is referred to the web version of this article.)

Table 2
UV-C doses assessed for their antiviral activity on car upholstery (porous surface) with recorded UV-C irradiances, exposure times and environmental conditions (relative humidity, temperature). Corresponding antiviral activity (M_v) and percentage of viral activity reduction ($R_{\%}$) are presented as mean ± standard deviation.

Sample	Dose (mJ/cm²)	Irradiance (mW/cm²)	Exposure time (min:s)	RH (%)	Temperature (°C)	M_v	$R_{\%}$ (%)
Car upholstery (polyester, nylon, foam)	7	0.20	0:38	47–58	21–22	0.15 ± 0.06	28.57 ± 10.67
	11	0.21	0:56	47–51	21–22	0.32 ± 0.05	51.52 ± 5.60
	22	0.23	1:50	45–57	19–22	0.42 ± 0.08	61.61 ± 6.86
	33	0.23	2:51	51–52	20–21	0.69 ± 0.07	79.20 ± 3.19
	66	0.24	5:11	52–53	20–21	0.81 ± 0.08	84.40 ± 2.59
	132	0.24	9:46	50–51	20–21	0.98 ± 0.07	89.39 ± 1.71
	198	0.24	14:06	44–45	22–23	1.17 ± 0.10	93.06 ± 1.53
	264	0.24	17:55	43–44	22–23	1.46 ± 0.18	96.17 ± 1.65
	330	0.24	23:09	47–49	22–23	1.61 ± 0.20	97.25 ± 1.27
	396	0.24	27:53	43–45	22–23	1.97 ± 0.30	98.68 ± 0.82
	462	0.24	31:30	44–45	21–22	2.01 ± 0.39	98.60 ± 1.10
	528	0.24	36:32	44–46	21–22	2.01 ± 0.00	99.03 ± 0.00

RH – Relative humidity.

non-porous surfaces. Moreover, this dosage was sufficient to reach the method's viral detection limit (*i.e.*, no active viral particles were recovered after the UV-C treatment) for 5 of 8 tested surfaces: glass, stainless steel, ceramic, polyvinyl chloride and polymethyl methacrylate. Even though infectious virus particles were still recovered after this treatment for waterproofed Aegean oak, polycarbonate, and glass, their reduction was always above 99.9%.

Considering the different compositions of the remaining porous samples tested in this phase, inactivation assays were performed with three pre-selected critical doses, enabling a broader evaluation of each sample: *i)* 132 mJ/cm², minimum dose for 1-log reduction of viral activity on reference porous surface ($R_{\%}$: 89.39 ± 1.71; Table 2); *ii)* 264 mJ/cm², intermediate dose; and, *iii)* 396 mJ/cm², minimum dose for 2-log reduction ($R_{\%}$: 98.68 ± 0.82, Table 2).

All experimental conditions and inactivation results are summarised and presented in Table 4 and Fig. 5. Fig. 5A demonstrates that doses of 132 mJ/cm² and 264 mJ/cm² (≈ 9- and 18-min exposure, respectively) guarantee 2-log and 3-log reduction of SARS-CoV-2 activity, respectively, on a tested public transportation upholstery. As shown in Fig. 5B, when using the pre-selected critical doses on synthetic leather, 132 mJ/cm² were already sufficient to ensure 3-log reduction of SARS-CoV-2 activity, reaching the detection limit of the method. Therefore, lower UV-C doses were tested (3, 8, 11, 33, and 66 mJ/cm²), demonstrating 2-log reduction being accomplished with 8 mJ/cm² (44 s exposure) and 3-log reduction with 11 mJ/cm² (≈ 1 min exposure).

The obtained results for hospital bed linen, depicted in Fig. 5C, demonstrate a minimum dose of 264 mJ/cm² (≈ 18 min exposure) is required to ensure 2-log SARS-CoV-2 activity reduction on this material. Moreover, it was enough to reach the method's detection limit, due to consistently low virus recovery rates, explained by the fact that cotton inherently presents good conditions to retain particles (in case of viruses, either viable or unviable) in its structure, as previously demonstrated [25]. This fact limited our ability to infer on the critical dose necessary to obtain a 99.9% reduction of viral activity. To overcome this limitation and confirm that low recovery rates were caused by intrinsic tissue characteristics, these assays were repeated using an increased (2×) inoculum (Table S2 and Fig. S3). The results show consistently low recovery rates and, although a guaranteed 2-log reduction was achieved with a lower dose (132 mJ/cm²), no 3-log reduction was demonstrated, due to the method's detection limit.

Our results for two clothing fabrics are shown in Fig. 5D-E. The findings for clothing fabric #1 (Fig. 5D) demonstrate that 132 mJ/cm² (≈ 9 min exposure) ensure 1-log reduction of SARS-CoV-2 activity. However, with the remaining pre-selected dosages (264 and 396 mJ/

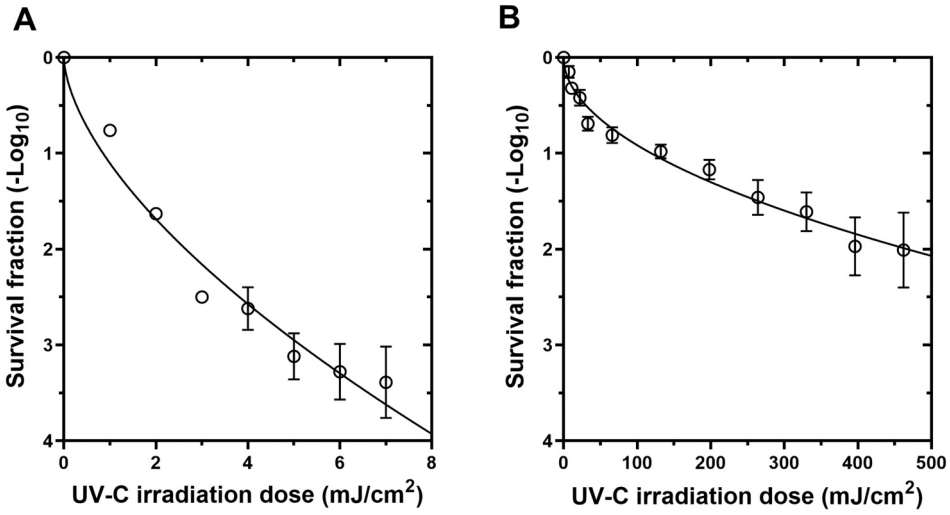

Fig. 4. Inactivation kinetics of SARS-CoV-2 promoted by UV-C radiation. Survival values are presented for: (A) polystyrene and (B) car upholstery. Data are presented as mean ± standard deviation. Non-linear regression applied to the inactivation kinetics data yielded LD_{90} and T values of 0.85 mJ/cm^2 and 0.61, respectively, for polystyrene ($R^2 = 0.97$), and 119.2 mJ/cm^2 and 0.51, respectively, for car upholstery ($R^2 = 0.98$).

Table 3
Antiviral activity of 8 mJ/cm^2 UV-C dosage on different non-porous surfaces, with recorded UV-C irradiances, exposure times and environmental conditions (relative humidity, temperature). Corresponding antiviral activity (M_v) and percentage of viral activity reduction ($R_{\%}$) are presented as mean ± standard deviation. Recovered infectious particles in control samples are presented in %.

Sample	Irradiance (mW/cm^2)	Exposure time (s)	RH (%)	Temperature (°C)	M_v	$R_{\%}$ (%)	Recovery rate (%)
PC	0.20	46	56–57	20–21	3.24 ± 0.23	99.94 ± 0.03	75
PMMA	0.21	43	46–47	21–22	>3.60*	>99.98*	93
PETG	0.20	45	55–56	20–21	3.41 ± 0.22	99.96 ± 0.03	78
Glass	0.23	38	46–47	25–26	>3.77*	>99.98*	100
Stainless steel	0.20	44	58–59	22–23	>3.56*	>99.97*	76
Waterproofed Aegean oak	0.24	36	58–59	24–25	3.60 ± 0.2	99.97 ± 0.02	100
Homogeneous PVC covering	0.21	42	58–59	19–20	>3.47*	>99.97*	59
Ceramics	0.21	42	47–48	21–22	>3.62*	>99.98*	97

RH – Relative humidity; PC – polycarbonate; PMMA – polymethyl methacrylate; PETG – polyethylene terephthalate glycol; PVC – polyvinyl chloride; * – No infectious virus particles were recovered after UV-C treatment, a value above the detection limit was assumed.

cm^2) no 2-log or 3-log reductions were achieved. Therefore, the highest assessed dose for the reference material (528 mJ/cm^2, exposure time > 37 min; Fig. 3) was included for testing, yet no 2-log nor 3-log reduction was guaranteed, as virus recovery rates remained low. The results obtained for clothing fabric #2 (Fig. 5E) demonstrate that the pre-selected dose of 264 mJ/cm^2 is not enough to ensure 2-log reduction, while a dose of 396 mJ/cm^2 is already sufficient to guarantee 3-log reduction, reaching the method's detection limit. Thus, to determine the critical dose necessary to obtain 2-log reduction of SARS-CoV-2 activity, an additional intermediate dose of 330 mJ/cm^2 was tested. Yet, no guaranteed 2-log reduction was achieved, implying a dosage between 330 and 396 mJ/cm^2 (exposure time between 23 and 26 min) is necessary.

Overall, these results highlight an efficient and rapid inactivation (<1 min) of at least 99.9% of infectious virus particles for all tested non-porous surfaces, but also that the effectiveness of UV-C treatment on porous surfaces is highly variable and composition-dependent.

4. Discussion

Direct absorption of UV-C radiation by viral nucleic acids and/or proteins leads to the generation of photoproducts and, consequently, to viral inactivation [7,26]. This highlights UV-C radiation as an economical, effective, and eco-friendly broad-spectrum antiviral tool. Nonetheless, 254 nm UV-C-based inactivation methods have limitations, which should be considered when interpreting the results. Material degradation can occur when multiple UV-C irradiation cycles of the same surface/material are required [23,27,28]. When treating materials with inner layers (porous surfaces), shadowing can take place, which decreases its germicidal effectiveness. Although discussed in several studies, only few [29–31] present possible solutions, such as UV-C irradiation setup adjustments to increase exposure or internal reflection. Moreover, health hazards associated to UV-C radiation exposure [32,33] need to be considered.

Previous studies demonstrated the effectiveness of 254 nm UV-C radiation against SARS-CoV-2 [8–16]. However, more coherent, and comprehensive datasets for its application on different surface compositions are needed. In this work, our aim was to generate complete datasets guaranteeing efficient SARS-CoV-2 inactivation on surfaces present in real-life environments. These can be used as reference for commercial viral inactivation equipment already available on the market or soon to be commercialized. To do so, we have assessed virus infectivity after UV-C exposure on different porous and non-porous surfaces (Table S1; Figs. S1-S2), using a clinical SARS-CoV-2 isolate.

Our first goal was to establish an experimental UV-C irradiation setup allowing a result extrapolation to real-life conditions. Therefore, particular attention was paid to keep experimental conditions equal while monitoring temperature and relative humidity. To ensure equal UV-C irradiance delivery [34], the UV-C lamp was placed at the same height, centrally above the samples and the UV-C sensor (Fig. 1A-B).

Initiating the UV-C inactivation studies, reference samples from each surface category were selected, and the decrease of infectious particle numbers evaluated as a function of the increase of UV-C dose. Reference

Table 4
UV-C doses assessed for their antiviral activity on tested porous surfaces with recorded UV-C irradiances, exposure times and environmental conditions (relative humidity, temperature). Corresponding antiviral activity (M_v) and percentage of viral activity reduction ($R_{\%}$) are presented as mean ± standard deviation. Recovered infectious particles in control samples are presented in %.

Sample	Dose (mJ/cm^2)	Irradiance (mW/cm^2)	Exposure time (min:s)	RH (%)	Temperature (°C)	M_v	$R_{\%}$ (%)	Recovery rate (%)
Bus upholstery	132	0.25	9:27	37–62	18–24	2.69 ± 0.46	99.67 ± 0.27	54–60
	264	0.24	18:08			>3.11*	>99.92*	
	396	0.24	28:22			>3.11*	>99.92*	
Synthetic leather	3	0.19	0:18	53–62	18–21	1.76 ± 0.09	98.24 ± 0.36	63
	8	0.20	0:44			2.73 ± 0.41	99.74 ± 0.16	
	11	0.20	1:02			>3.31*	>99.95*	
	33	0.22	2:43			>3.31*	>99.95*	
	66	0.24	5:07			>3.31*	>99.95*	
	132	0.25	9:27	53–61	19–21	>3.18*	>99.93*	85
	264	0.24	18:08			>3.18*	>99.93*	
	396	0.24	28:22			>3.18*	>99.93*	
Hospital bed linen	132	0.24	9:28	53–59	18–21	1.98 ± 0.31	98.50 ± 1.61	4–6
	264	0.24	18:16			>2.18*	>99.34*	
	396	0.25	28:09			>2.18*	>99.34*	
Clothing fabric #1	132	0.24	9:23	52–66	18–21	1.67 ± 0.18	97.68 ± 0.79	39–52
	264	0.24	18:08			1.87 ± 0.26	98.39 ± 0.86	
	396	0.24	27:23			1.81 ± 0.11	98.40 ± 0.41	
	528	0.24	37:00			2.16 ± 0.57	98.79 ± 0.79	
Clothing fabric #2	132	0.24	9:20	47–75	21–25	1.44 ± 0.07	96.29 ± 0.61	84
	264	0.24	17:33			1.60 ± 0.13	97.40 ± 0.68	
	330	0.24	22:46			1.89 ± 0.17	98.61 ± 0.46	
	396	0.25	25:58			>3.31*	>99.95*	

RH – Relative humidity; * – No infectious virus particles were recovered after UV-C treatment, a value above the detection limit was assumed.

samples were selected either due to the widespread use in everyday items, such as packaging material or household appliances (polystyrene, non-porous), or the challenging composition and thickness regarding anticipated shadowing events during UV-C treatment (car upholstery, porous). Figs. 2 and 3 demonstrate that higher irradiation doses (and consequently longer exposure times) increase viral inactivation on the selected surfaces, confirmed by a strong positive correlation (r_s of 0.993 and 0.994 for car upholstery and polystyrene, respectively). As the assay's detection limit was reached in most cases, the assessment of correlation intensities is limited. Nevertheless, our data show that UV-C irradiation rapidly and effectively inactivates SARS-CoV-2 on non-porous and porous surfaces. Still, on car upholstery samples the required dose (528 mJ/cm^2, Fig. 3) to achieve a 2-log reduction (99%) of viral activity was 176-fold higher compared to polystyrene (3 mJ/cm^2, Fig. 2), demonstrating that an efficient infectious particle reduction is achieved faster and at lower doses on non-porous surfaces.

The UV-C studies performed with the remaining selected materials demonstrated that the dose required to achieve 2-log reduction in viral activity on porous surfaces with low cotton percentages, *i.e.*, bus upholstery (20–35% cotton, Table S1; 132 mJ/cm^2, Table 4), was 44-fold higher than on non-porous surfaces (3 mJ/cm^2; Table 1). For fabrics with higher cotton percentages, like clothing fabric #1 and hospital bed linen (65 and 100% cotton, respectively; Table S1), this difference increases up to 176-fold (Table 4), explained by the natural ability of cotton to retain particles in its structure [25]. Resultant low virus recovery rates limit the capacity to assess respective critical doses necessary to reduce viral activity by 99.9%. Future studies should aim to improve virus recovery protocols for materials with high cotton content. A 3-log reduction in viral activity on materials with low cotton percentages, such as bus upholstery (264 mJ/cm^2) and clothing fabric #2 (396 mJ/cm^2) is reached after a minimum treatment of 18 and 25 min, respectively (Table 4). The same reduction on all tested non-porous surfaces (Tables 1 and 3) is achieved considerably faster (<1 min), justified by fundamental issues related to shadowing, sample retention and effective UV-C dose delivery on porous materials, as previously discussed. Although synthetic leather was initially regarded as a porous surface, its behaviour is comparable to non-porous surfaces, as a 3-log reduction of infectious virions is achieved within 1 min (≥11 mJ/cm^2, Table 4). This can be explained by the low absorption capacity of its top layer compound (100% PVC; Table S1). Our results demonstrate that UV-C treatment effectiveness is highly variable and composition-dependent, emphasizing the need for customization according to individual surface properties.

Environmental conditions, such as temperature and humidity, can influence the response of SARS-CoV-2 to UV-C irradiation [19,20] and were therefore evaluated during our experiments. Results from Tables 1 and 2 suggest that assays carried out at lower temperatures (20–21°C) and relative humidity (40–50%) tend to present lower standard deviations, when compared to those carried out at higher humidity and temperature. Nevertheless, these finding should be further investigated.

In conclusion, our results will support the development of new UV-C-based devices and the optimization of existing technologies, enabling customizable, surface-dependent inactivation protocols, ensuring higher antiviral efficiencies. For instance, extrapolating from our results, a UV-C lamp setup with 0.119 W placed 2 m from the surface, can achieve a 99.9% reduction of viable SARS-CoV-2 within 1 min for an area of 16 m^2 composed of non-porous materials listed in Table 3. For porous materials with low to no cotton percentage (bus upholstery and clothing fabric #2), the disinfection time for the same area increases to 23 and 39 min, respectively.

These and other findings support that, if properly applied, UV-C radiation is an economical, effective, and eco-friendly broad-spectrum antiviral tool, very powerful in the current fight against COVID-19. It can be applied in a wide range of public institutions, including hospitals, nursing homes, workplaces, schools, airports, and shopping centres, to disinfect contaminated surfaces/equipment to prevent and reduce SARS-CoV-2 contact transmission.

Funding

This work was developed within the UVtizer project, constituted by the consortium Castros, MATGLOW, CeNTI & iMM, supported by COMPETE 2020 and Portugal 2020 through ERDF (grant number POCI-01-02B7-FEDER-062110). P.M.S. acknowledges fellowship SFRH/BD/118413/2016 from Fundação para a Ciência e a Tecnologia – Ministério da Ciência, Tecnologia e Ensino Superior (FCT-MCTES, Portugal).

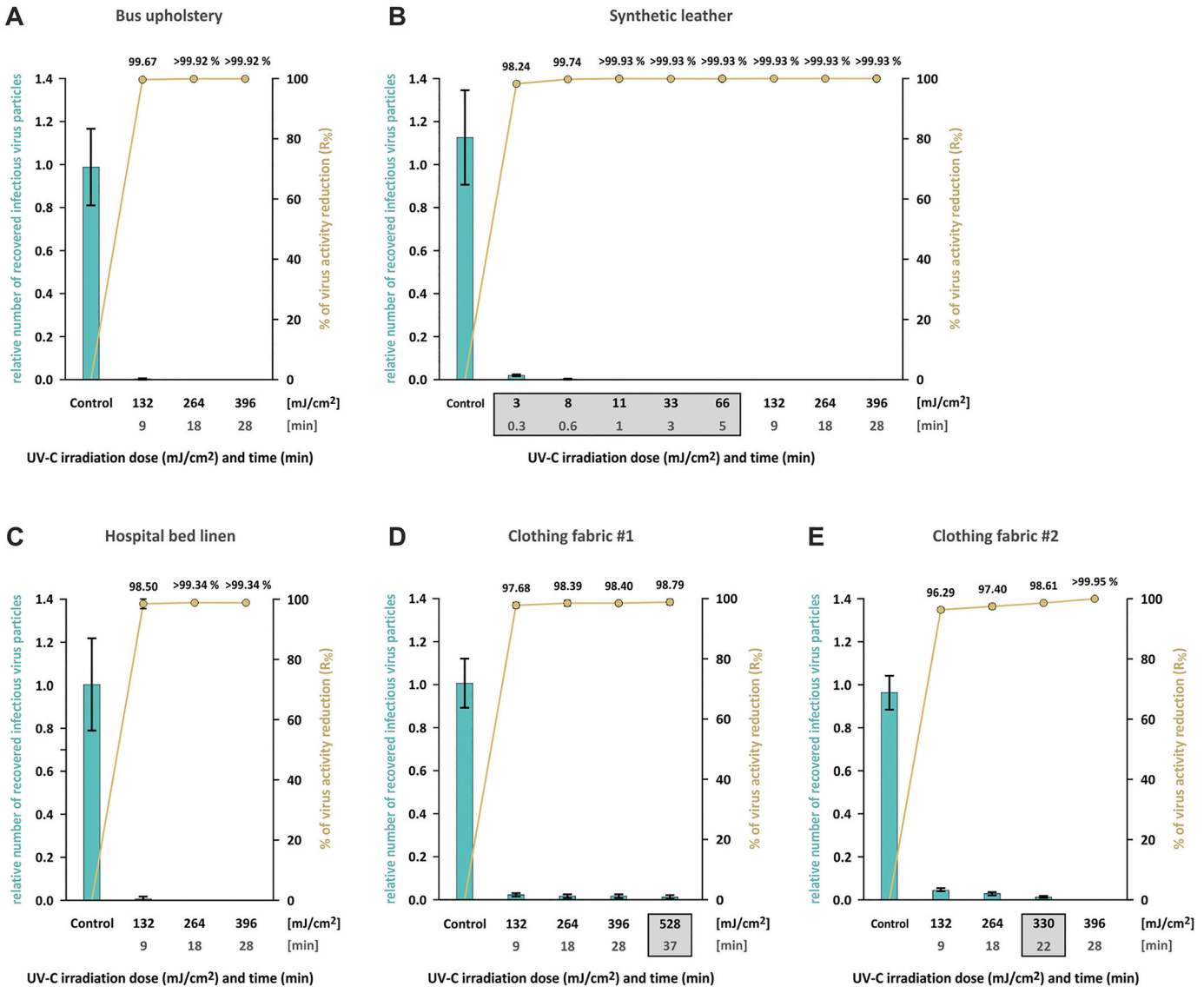

Fig. 5. Inactivation results using critical doses of 132, 264 and 396 mJ/cm^2 on tested porous surfaces: (A) bus upholstery, (B) synthetic leather, (C) hospital bed linen, (D) clothing fabric #1 and (E) #2. Bars represent infectious virus particle numbers recovered from the sample after respective irradiation times in relation to the control (no UV-C exposure). Yellow dots and line represent corresponding percentages of viral inactivation. Additionally, analysed doses are highlighted in grey. Data are presented as mean ± standard deviation. (For interpretation of the references to colour in this figure legend, the reader is referred to the web version of this article.)

CRediT authorship contribution statement

Ana L. Tomás: Conceptualization, Methodology, Investigation, Writing – original draft. **Anna Reichel:** Conceptualization, Methodology, Investigation, Writing – original draft. **Patrícia M. Silva:** Conceptualization, Methodology, Investigation, Writing – original draft. **Pedro G. Silva:** Conceptualization, Methodology, Writing – review & editing. **João Pinto:** Conceptualization, Methodology. **Inês Calado:** Conceptualization, Methodology. **Joana Campos:** Conceptualization, Methodology. **Ilídio Silva:** Conceptualization, Methodology. **Vasco Machado:** Conceptualization, Methodology. **Roberto Laranjeira:** Conceptualization, Methodology. **Paulo Abreu:** Resources, Conceptualization, Methodology, Writing – review & editing. **Paulo Mendes:** Resources, Conceptualization, Methodology, Writing – review & editing. **Nabiha Ben Sedrine:** Resources, Conceptualization, Methodology, Writing – review & editing. **Nuno C. Santos:** Conceptualization, Methodology, Writing – review & editing, Supervision.

Declaration of Competing Interest

The authors declare no conflict of interest.

Acknowledgments

Authors thank the Biosafety Level 3 Facility of Instituto de Medicina Molecular (iMM) for their services and assistance, as well as to iMM Technology Transfer Office for fostering this Industry-Academia collaboration. Authors are grateful to all suppliers who kindly provided surface samples for testing: TMG_Famalicão, Rosinha – Produtos Industriais, CITEVE, Gaia Chapa, FINSA, and LOVE ceramics tiles. Authors thank Prof. Pedro Simas Lab (iMM) for providing the initial SARS-CoV-2 clinical isolate, and to Dr. Caetano P. Sabino (BioLambda, Scientific and Commercial LTD, São Paulo, Brazil) for valuable suggestions.

Appendix A. Supplementary data

Supplementary data to this article can be found online at https://doi.org/10.1016/j.jphotobiol.2022.112531.

References

[1] N. van Doremalen, T. Bushmaker, D.H. Morris, et al., Aerosol and surface stability of SARS-CoV-2 as compared with SARS-CoV-1, N. Engl. J. Med. 382 (2020) 1564–1567, https://doi.org/10.1056/NEJMc2004973.

[2] G. Kampf, D. Todt, S. Pfaender, et al., Persistence of coronaviruses on inanimate surfaces and their inactivation with biocidal agents, J. Hosp. Infect. 104 (2020) 246–251, https://doi.org/10.1016/j.jhin.2020.01.022.

[3] A.W.H. Chin, J.T.S. Chu, M.R.A. Perera, et al., Stability of SARS-CoV-2 in different environmental conditions, Lancet Microbe. 1 (4) (2020), e145, https://doi.org/10.1016/S2666-5247(20)30003-3.

[4] F.J. García de Abajo, R.J. Hernández, I. Kaminer, et al., Back to normal: an old physics route to reduce SARS-CoV-2 transmission in indoor spaces, ACS Nano. 14 (7) (2020) 7704–7713, https://doi.org/10.1021/acsnano.0c04596.

[5] B.H. Ryu, Y. Cho, O.H. Cho, S.I. Hong, et al., Environmental contamination of SARS-CoV-2 during the COVID-19 outbreak in South Korea, Am. J. Infect. Control. 48 (8) (2020) 875–879, https://doi.org/10.1177/17571774211033348.

[6] P.Y. Chia, K.K. Coleman, Y.K. Tan, et al., Detection of air and surface contamination by SARS-CoV-2 in hospital rooms of infected patients, Nat. Commun. 11 (1) (2020) 2800, https://doi.org/10.1038/s41467-020-16670-2.

[7] C.W. Lo, R. Matsuura, K. Iimura, et al., UVC disinfects SARS-CoV-2 by induction of viral genome damage without apparent effects on viral morphology and proteins, Sci. Rep. 11 (1) (2021) 13804, https://doi.org/10.1038/s41598-021-93231-7.

[8] S.E. Simmons, R. Carrion, K.J. Alfson, et al., Deactivation of SARS-CoV-2 with pulsed-xenon ultraviolet light: implications for environmental COVID-19 control, Infect. Control Hosp. Epidemiol. 42 (2) (2021) 127–130, https://doi.org/10.1017/ice.2020.399.

[9] C.S. Heilingloh, U.W. Aufderhorst, L. Schipper, et al., Susceptibility of SARS-CoV-2 to UV irradiation, Am. J. Infect. Control. 48 (2020) 1273–1275, https://doi.org/10.1016/j.ajic.2020.07.031.

[10] H. Kitagawa, T. Nomura, T. Nazmul, et al., Effectiveness of 222-nm ultraviolet light on disinfecting SARS-CoV-2 surface contamination, Am. J. Infect. Control. 49 (3) (2021) 299–301, https://doi.org/10.1016/j.ajic.2020.08.022.

[11] E. Criscuolo, R.A. Diotti, R. Ferrarese, et al., Fast inactivation of SARS-CoV-2 by UV-C and ozone exposure on different materials, Emerg. Microbes Infect. 10 (1) (2021) 206–210, https://doi.org/10.1080/22221751.2021.1872354.

[12] M. Lualdi, A. Cavalleri, A. Bianco, et al., Ultraviolet C lamps for disinfection of surfaces potentially contaminated with SARS-CoV-2 in critical hospital settings: examples of their use and some practical advice, BMC Infect. Dis. 21 (1) (2021), https://doi.org/10.1186/s12879-021-06310-5, 594-594.

[13] A. Gidari, S. Sabbatini, S. Bastianelli, et al., SARS-CoV-2 survival on surfaces and the effect of UV-C light, Viruses. 13 (3) (2021) 408, https://doi.org/10.3390/v13030408.

[14] M. Biasin, A. Bianco, G. Pareschi, et al., UV-C irradiation is highly effective in inactivating SARS-CoV-2 replication, Sci. Rep. 11 (1) (2021) 6260, https://doi.org/10.1038/s41598-021-85425-w.

[15] N. Storm, L.G. McKay, S.N. Downs, et al., Rapid and complete inactivation of SARS-CoV-2 by ultraviolet-C irradiation, Sci. Rep. 10 (1) (2020) 22421, https://doi.org/10.1038/s41598-020-79600-8.

[16] S. Ulloa, C. Bravo, E. Ramirez, et al., Inactivation of SARS-CoV-2 isolates from lineages B. 1.1. 7 (alpha), P. 1 (gamma) and B. 1.110 by heating and UV irradiation, J. Virol. Methods 295 (2021) 114216, https://doi.org/10.1016/j.jviromet.2021.114216.

[17] M.J. Matson, C.K. Yinda, S.N. Seifert, et al., Effect of environmental conditions on SARS-CoV-2 stability in human nasal mucus and sputum, Emerg. Infect. Dis. J. 26 (9) (2020) 2276–2278, https://doi.org/10.3201/eid2609.202267.

[18] B. Pastorino, F. Touret, M. Gilles, et al., Prolonged infectivity of SARS-CoV-2 in fomites, Emerg. Infect. Dis. J. 26 (9) (2020) 2256–2257, https://doi.org/10.3201/eid2609.201788.

[19] D.H. Morris, K.C. Yinda, A. Gamble, et al., Mechanistic theory predicts the effects of temperature and humidity on inactivation of SARS-CoV-2 and other enveloped viruses, eLife. 10 (2021), e65902, https://doi.org/10.7554/eLife.65902.

[20] E.R. Blatchley III, B. Petri, W. Sunc, SARS-CoV-2 UV dose-response behavior White paper, Int. Ultraviolet Associat. (2020), https://doi.org/10.6028/jres.126.018.

[21] J.B. Case, A.L. Bailey, A.S. Kim, et al., Growth, detection, quantification, and inactivation of SARS-CoV-2, Virology. 548 (2020) 39–48, https://doi.org/10.1016/j.virol.2020.05.015.

[22] UVSolutions [Internet], The Official Publication of the International Ultraviolet Association. UV Degradation Effects in Materials – An Elementary Overview, Available from: https://uvsolutionsmag.com/articles/2019/uv-degradation-effects-in-materials-an-elementary-overview/, 2019 Dec 12. accessed May 12, 2022.

[23] M. Moezzi, M. Ghane, The effect of UV degradation on toughness of nylon 66/polyester woven fabrics, J. Text. Inst. 104 (12) (2013) 1277–1283, https://doi.org/10.1080/00405000.2013.796629.

[24] C.P. Sabino, M. Wainwright, C. dos Anjos, F.P. Sellera, M.S. Baptista, N. Lincopan, et al., Inactivation kinetics and lethal dose analysis of antimicrobial blue light and photodynamic therapy, Photodiagn. Photodyn. Ther. 28 (2019) 186–191, https://doi.org/10.1016/j.pdpdt.2019.08.022.

[25] O. Sauperl, Textiles for protection against microorganism, in: AIP Conference Proceedings, AIP Publishing LLC, 2016, p. 020021, https://doi.org/10.1063/1.4945976.

[26] A. Ariza-Mateos, S. Prieto-Vega, R. Diaz-Toledano, et al., RNA self-cleavage activated by ultraviolet light-induced oxidation, Nucleic Acids Res. 40 (4) (2012) 1748–1766, https://doi.org/10.1093/nar/gkr822.

[27] M. Yujie, Z. Rae, R. Kurt, et al., Effect of ultraviolet C disinfection treatment on the nanomechanical and topographic properties of N95 respirator filtration microfibers, MRS Adv. 5 (2020) 2863–2872, https://doi.org/10.1557/adv.2020.347.

[28] J.S. Smith, H. Hanseler, J. Welle, et al., Effect of various decontamination procedures on disposable N95 mask integrity and SARS-CoV-2 infectivity, J. Clin. Transl. Sci. 5 (1) (2020), e10, https://doi.org/10.1017/cts.2020.494.

[29] G.R. Golovkine, A.W. Roberts, C. Cooper, et al., Practical considerations for ultraviolet-C radiation mediated decontamination of N95 respirator against SARS-CoV-2 virus, PLoS One. 16 (10) (2021), e0258336, https://doi.org/10.1371/journal.pone.0258336.

[30] R. Banerjee, P. Roy, S. Das, et al., A hybrid model integrating warm heat and ultraviolet germicidal irradiation might efficiently disinfect respirators and personal protective equipment, Am. J. Infect. Control. 49 (2021) 309–318, https://doi.org/10.1016/j.ajic.2020.07.022.

[31] R.M. Gilbert, M.J. Donzanti, D.J. Minahan, et al., Mask reuse in the COVID-19 pandemic: creating an inexpensive and scalable ultraviolet system for filtering facepiece respirator decontamination, Glob. Health Sci. Pract. 8 (2020) 582–595, https://doi.org/10.9745/GHSP-D-20-00218.

[32] A. Trevisan, S. Piovesan, A. Leonardi, et al., Unusual high exposure to ultraviolet-C radiation, Photochem. Photobiol. 82 (4) (2006) 1077–1079, https://doi.org/10.1562/2005-10-27-ra-728.

[33] D. Balasubramanian, Ultraviolet radiation and cataract, J. Ocul. Pharmacol. Ther. 16 (3) (2000) 285–297, https://doi.org/10.1089/jop.2000.16.285.

[34] D.R. Grimes, C. Robbins, N.J. O'Hare, Dose modeling in ultraviolet phototherapy, Med. Phys. 37 (10) (2010) 5251–5257, https://doi.org/10.1118/1.3484093.